Figure 1. Generic block diagram for generation of a PAM signal.
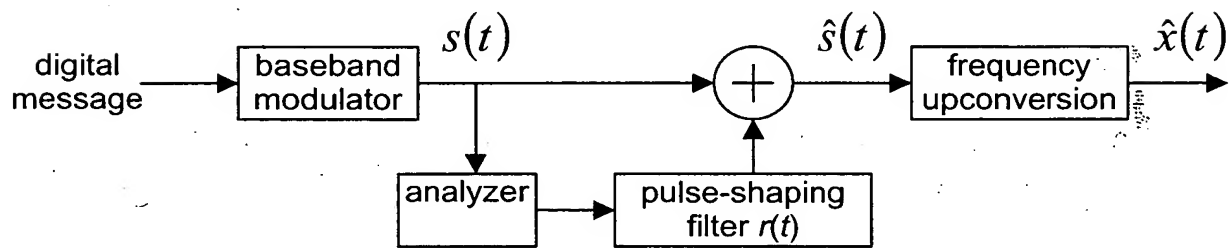

Figure 2a. Modification of generic PAM generator to include present invention.
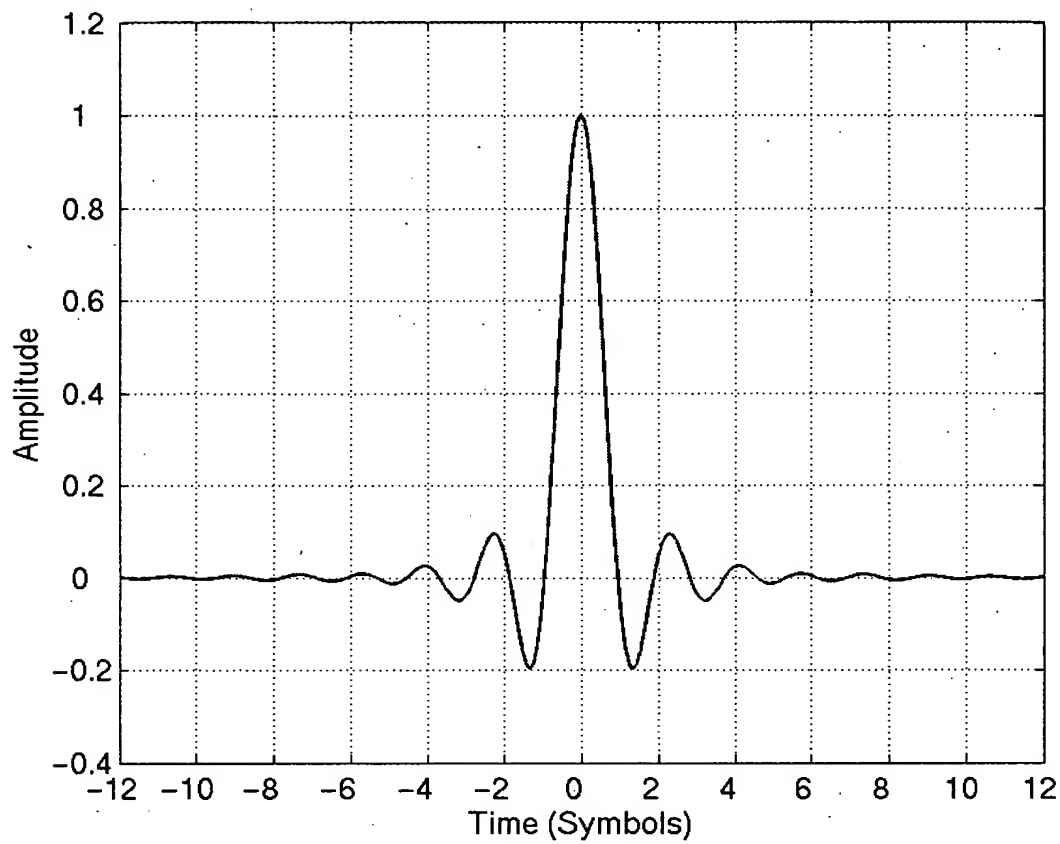
Figure 3. Impulse response of a square-root raised-cosine pulse shaping filter with 22% excess bandwidth.
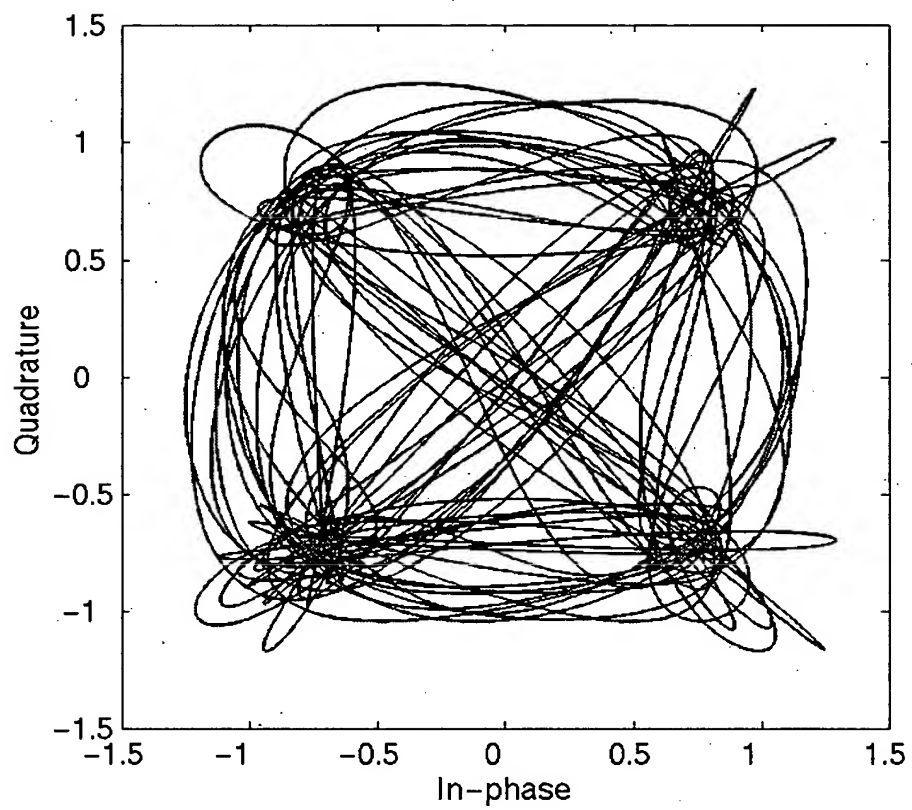
Figure 4. I-Q plot (vector diagram) of a portion of a QPSK signal with square-root raised-cosine pulse shaping.
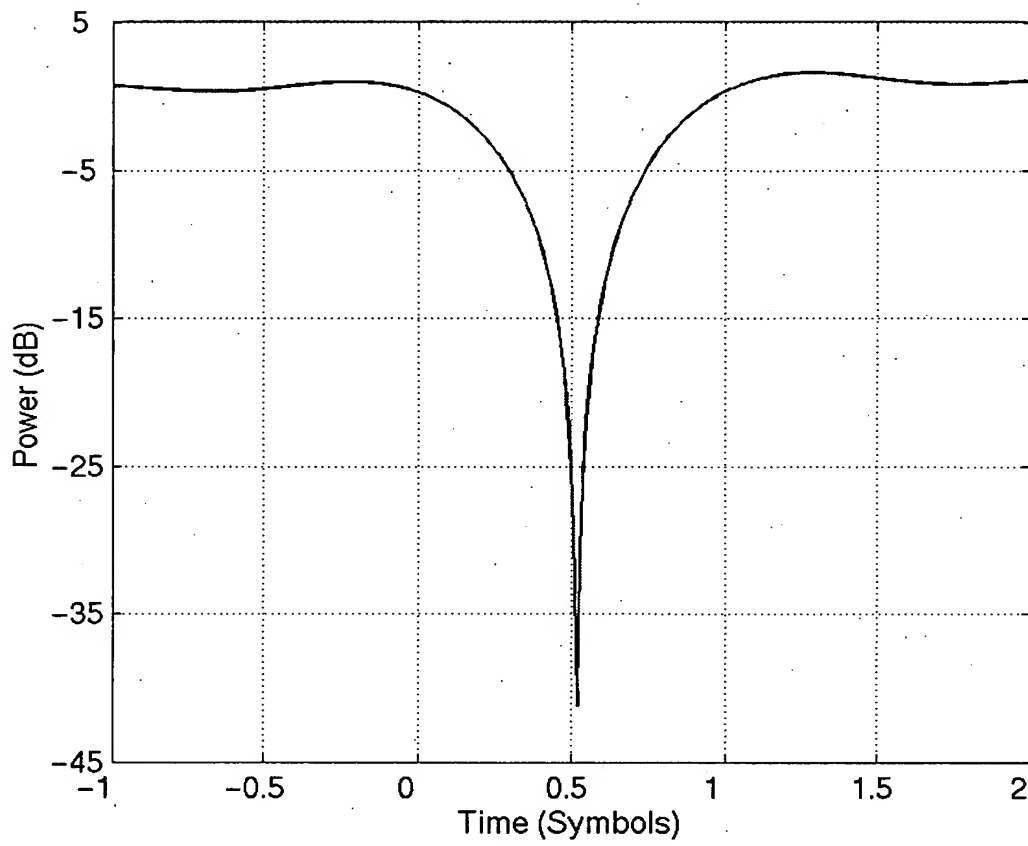
Figure 5. Brief section of power of the pulse-shaped QPSK signal as a function of time.
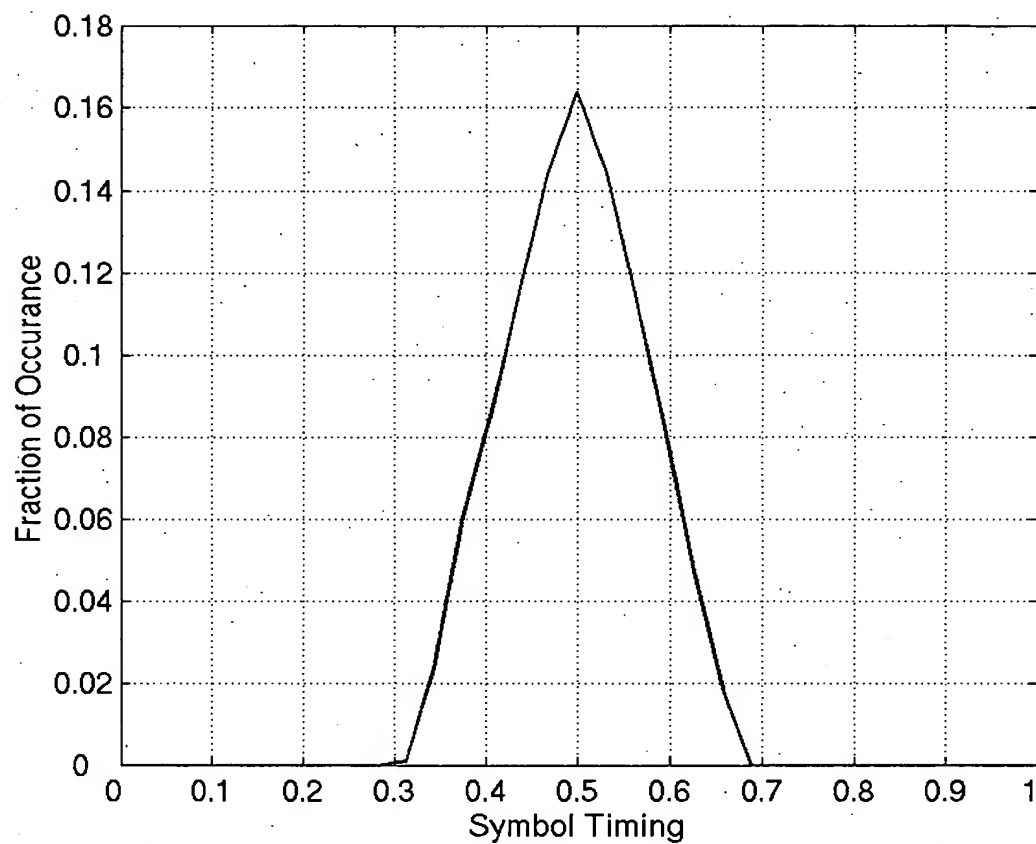
Figure 6. Histogram showing the temporal location of signal magnitude minima, including only those minima that are more than 12 dB below the mean power.
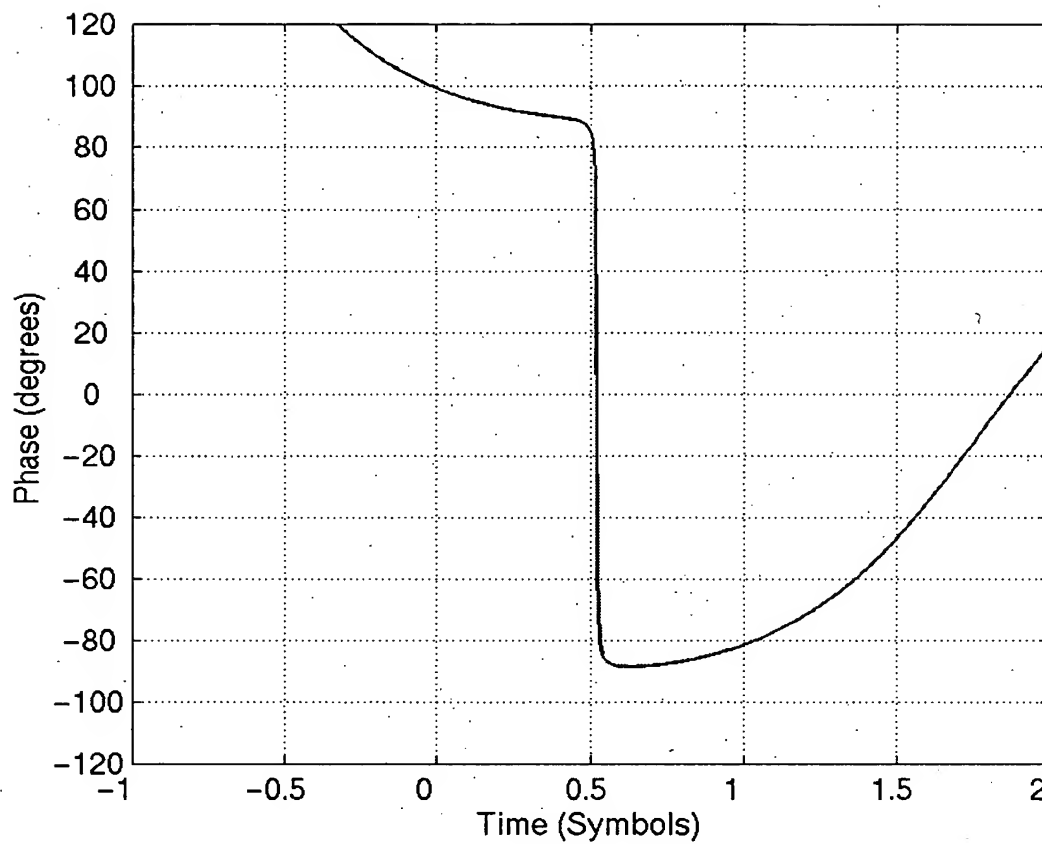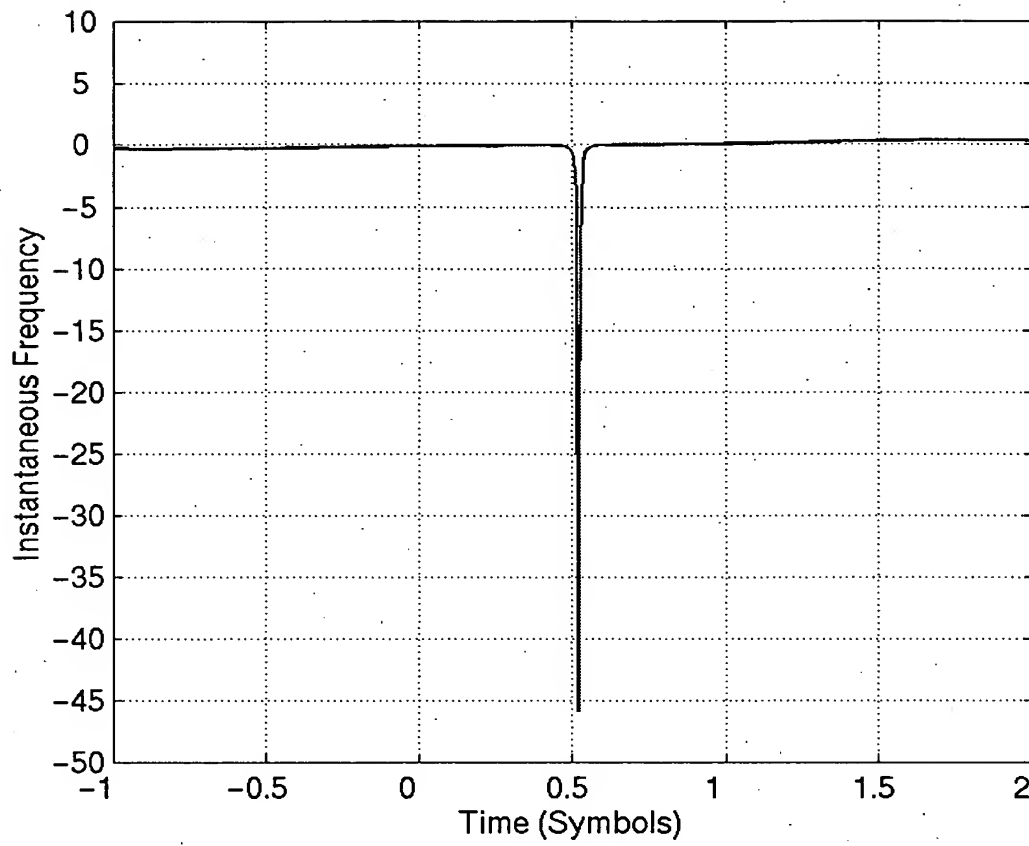
Figure 7. Phase of the QPSK signal as a function of time about an envelope minimum event.

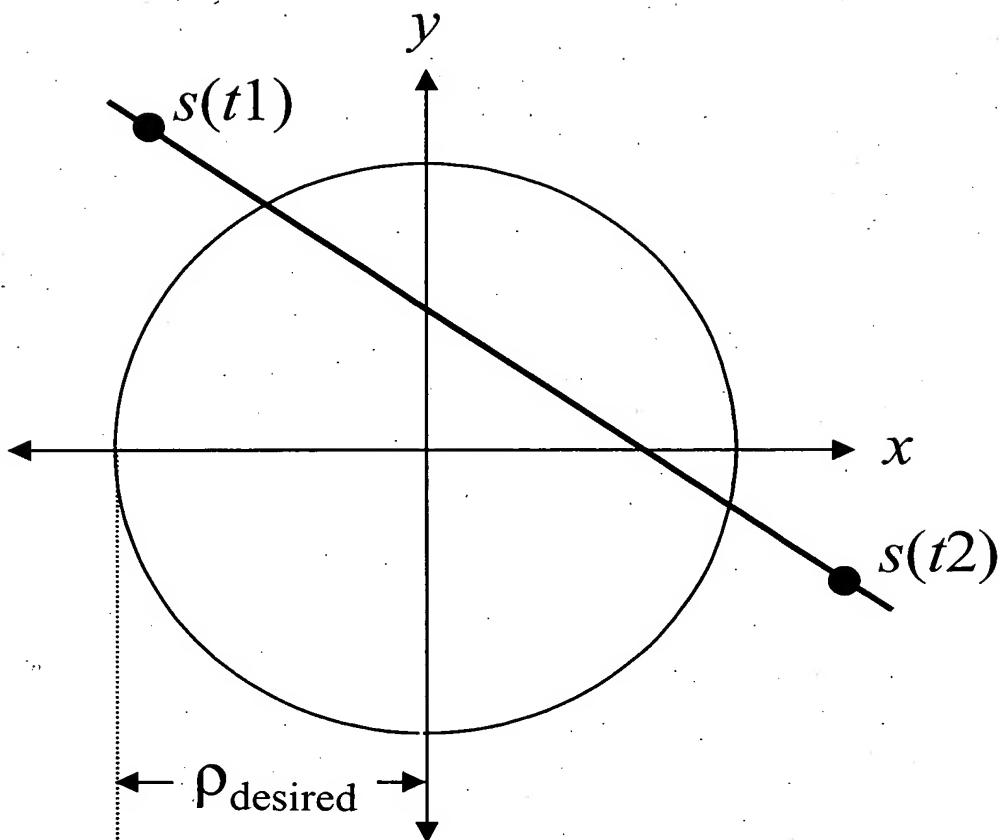**Figure 8.** Instantaneous frequency expressed as a multiple of the symbol rate for the signal of Figure 7.

Figure 9a. This figure illustrates a situation where the signal magnitude at discrete time indices t1 and t2 is greater than the desired minimum value $\rho_{desired}$. However, the magnitude of the continuous time waveform will clearly fall below the desired minimum value.
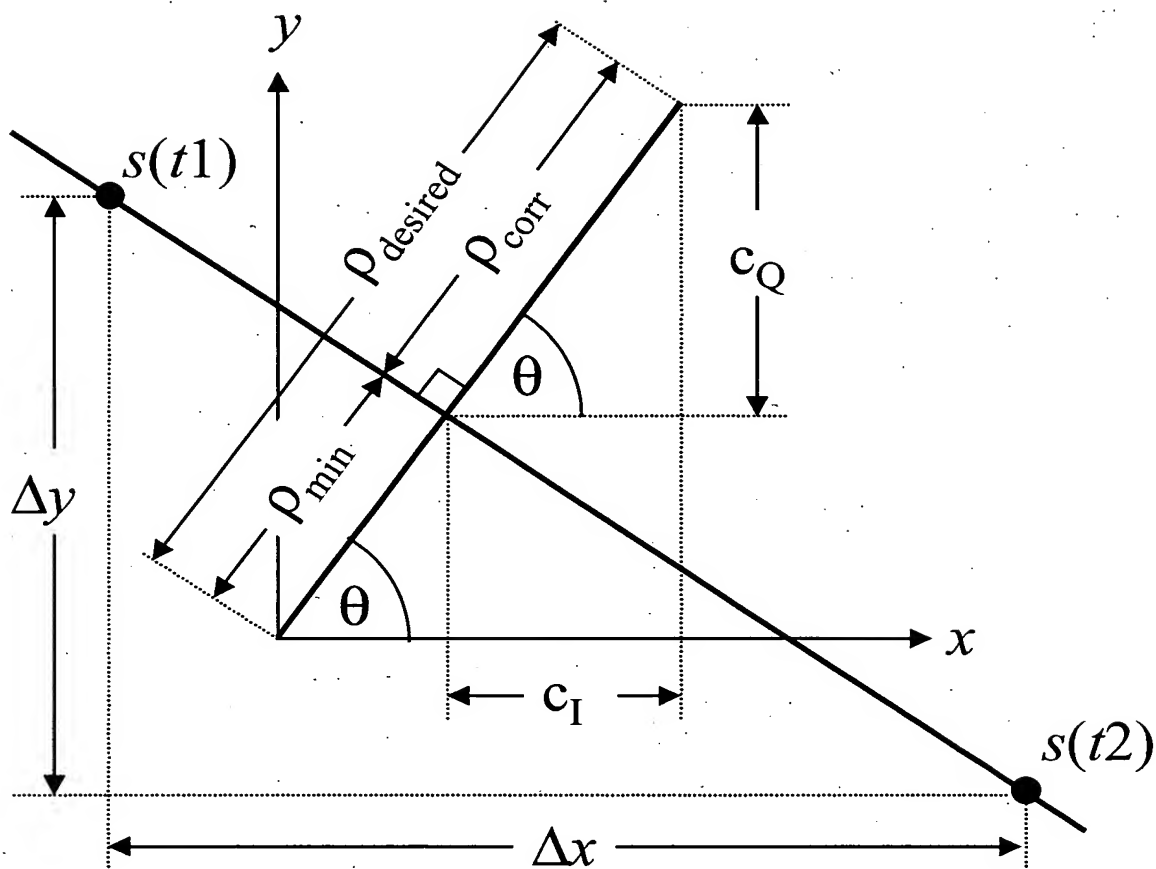
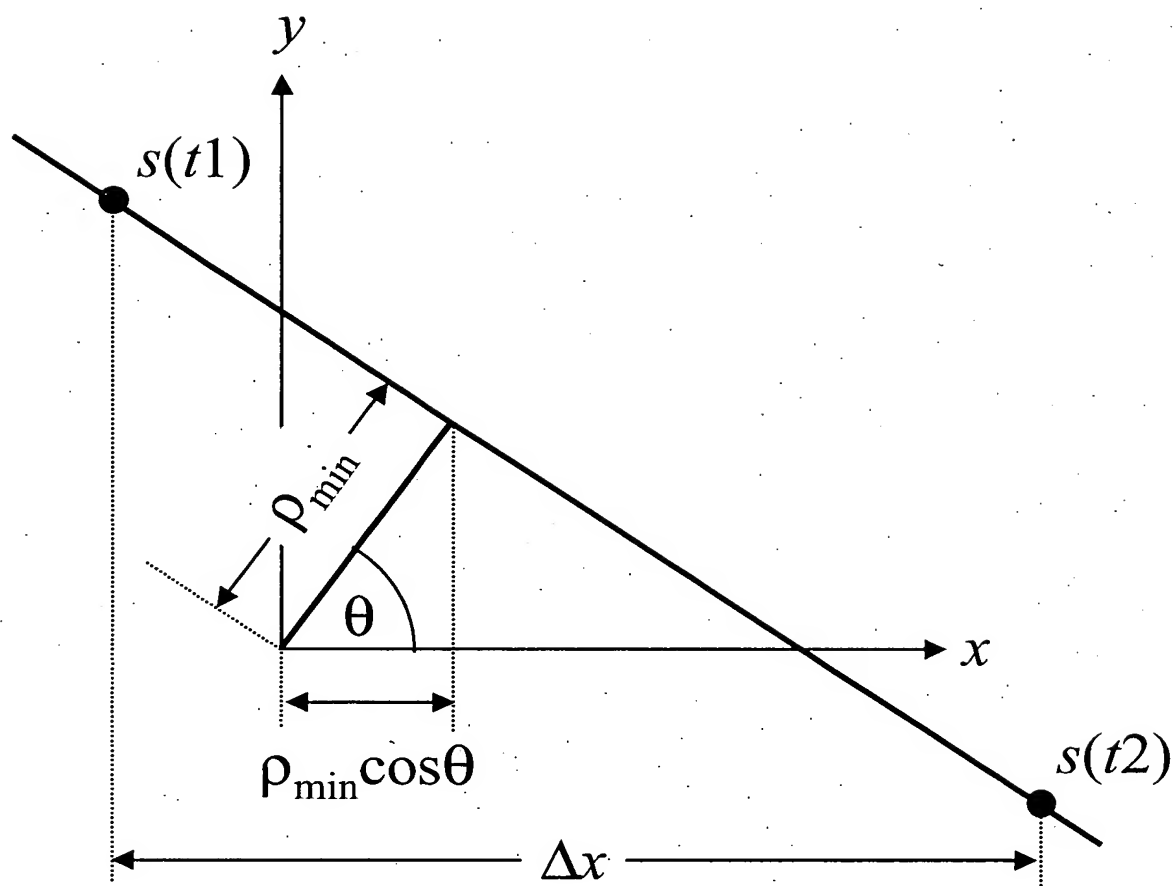Figure 9b. The locally linear model for the signal s(t)

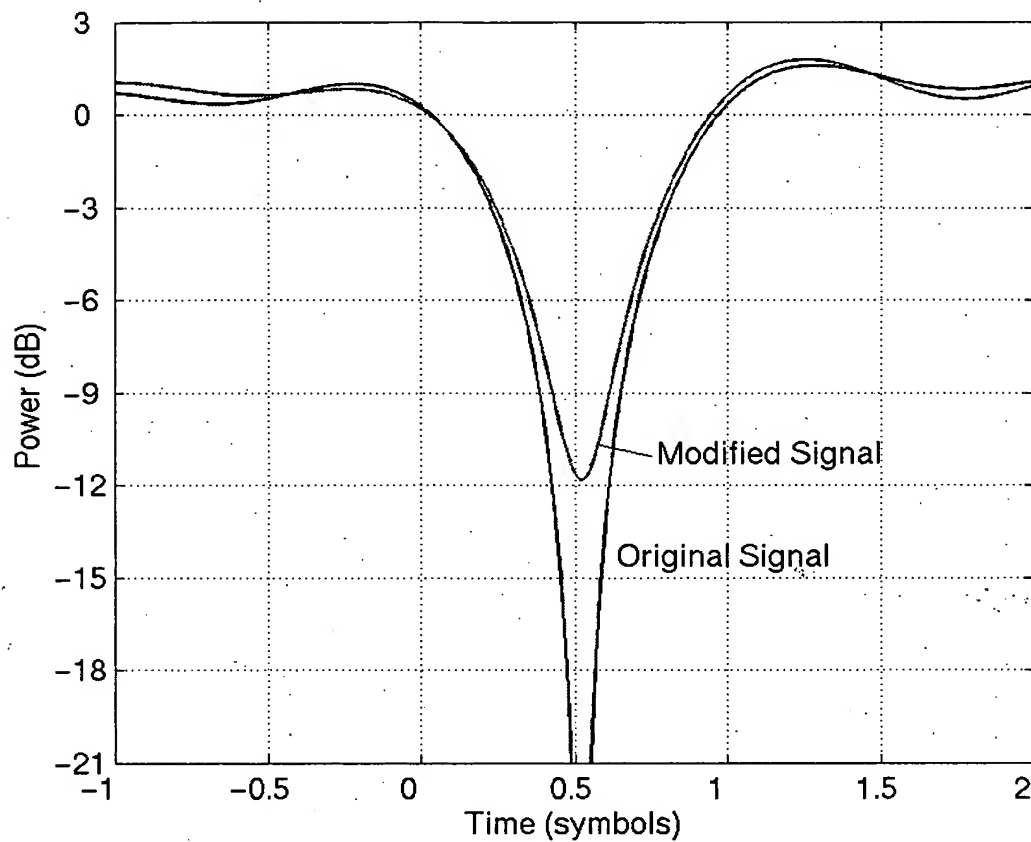Figure 9c. Calculation of t_min based on the locally linear model.

Figure 10 Comparison of the original signal power and the power of the signal after addition of a single, complex-weighted pulse designed to keep the minimum power above −12 dB of average signal power.
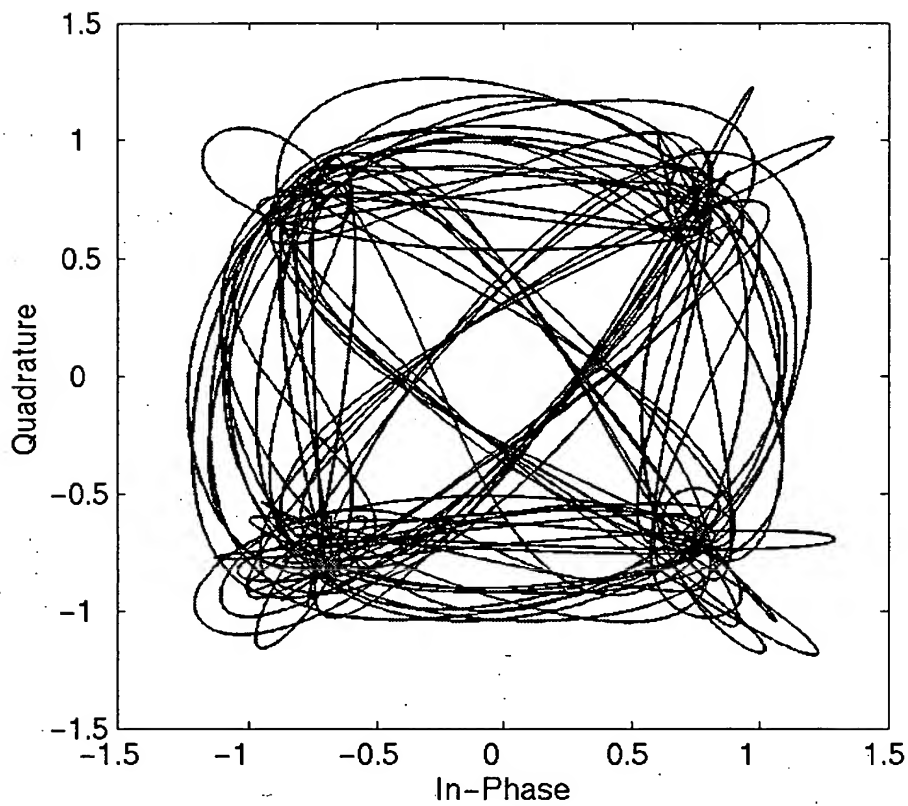
Figure 11 I-Q plot of a QPSK signal that has been modified to keep the instantaneous power greater than -12 dB relative to the RMS power.
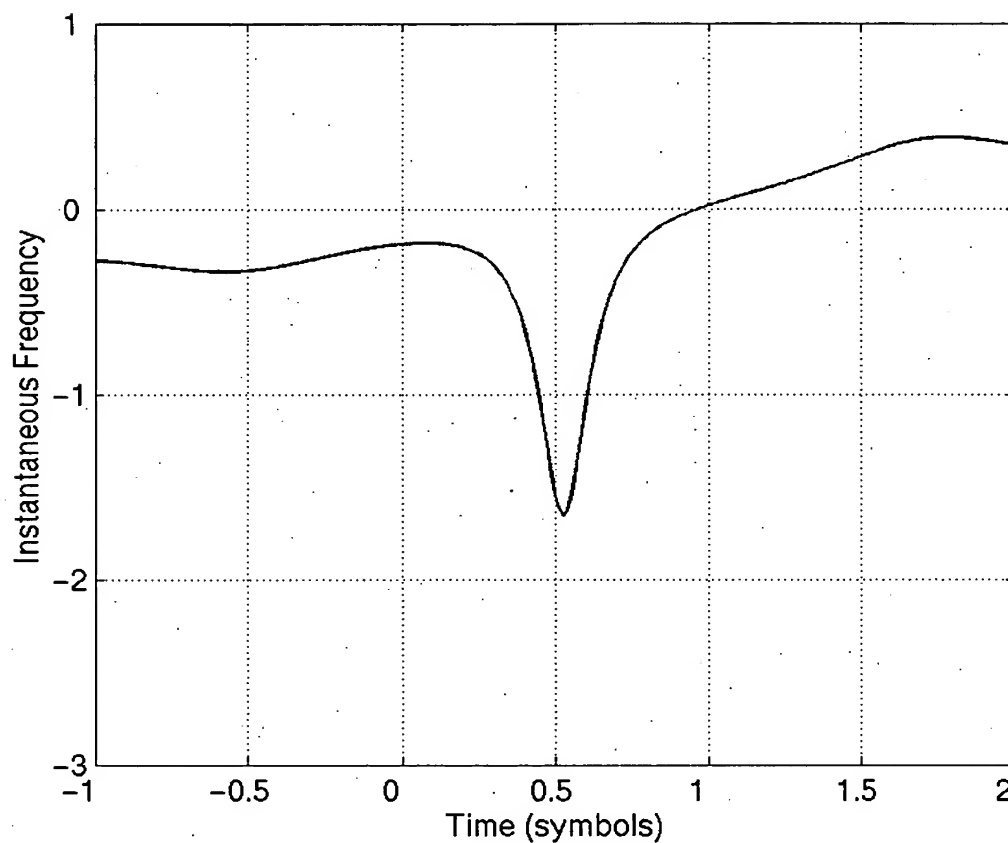
Figure 12 Instantaneous frequency of the modified signal of Figure 10, expressed as a multiple of the symbol rate.
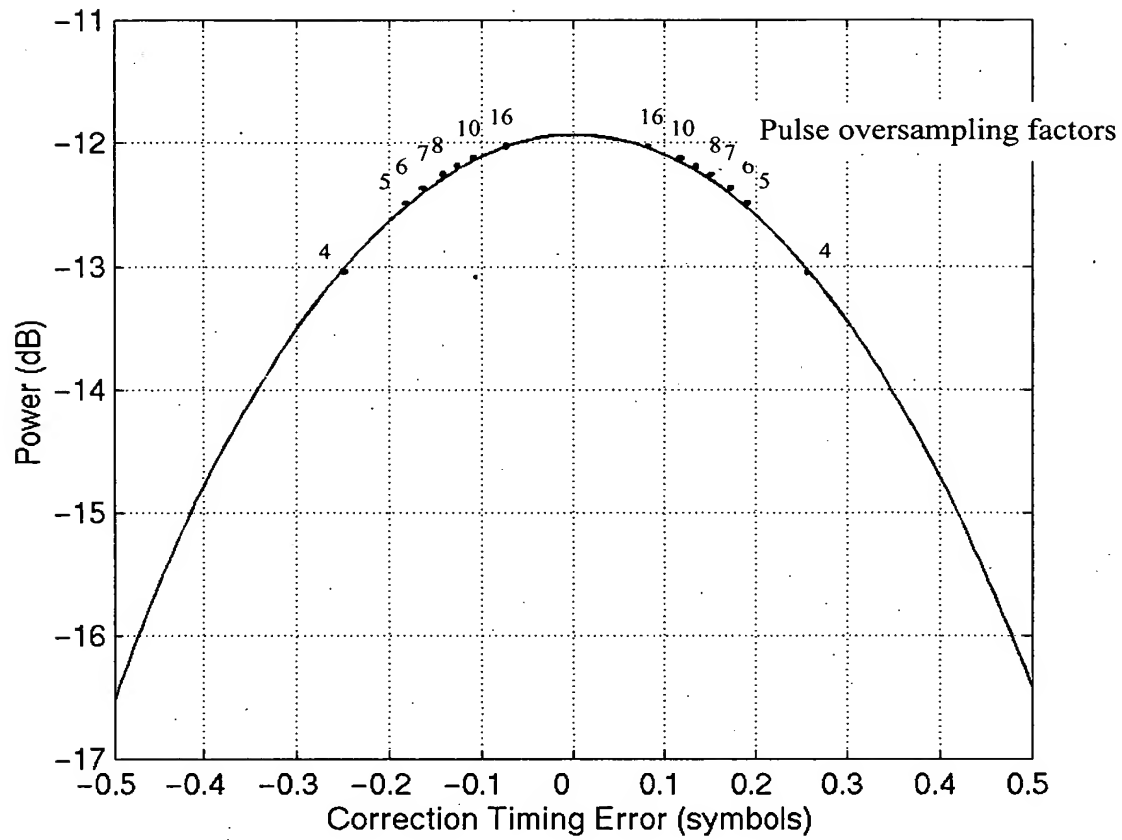
Figure 13. Minimum power in the modified signal as a function of error in the time at which the corrective pulse is added, where -12dB corresponds to the desired hole. The magnitude and phase of the corrective pulse are held constant.
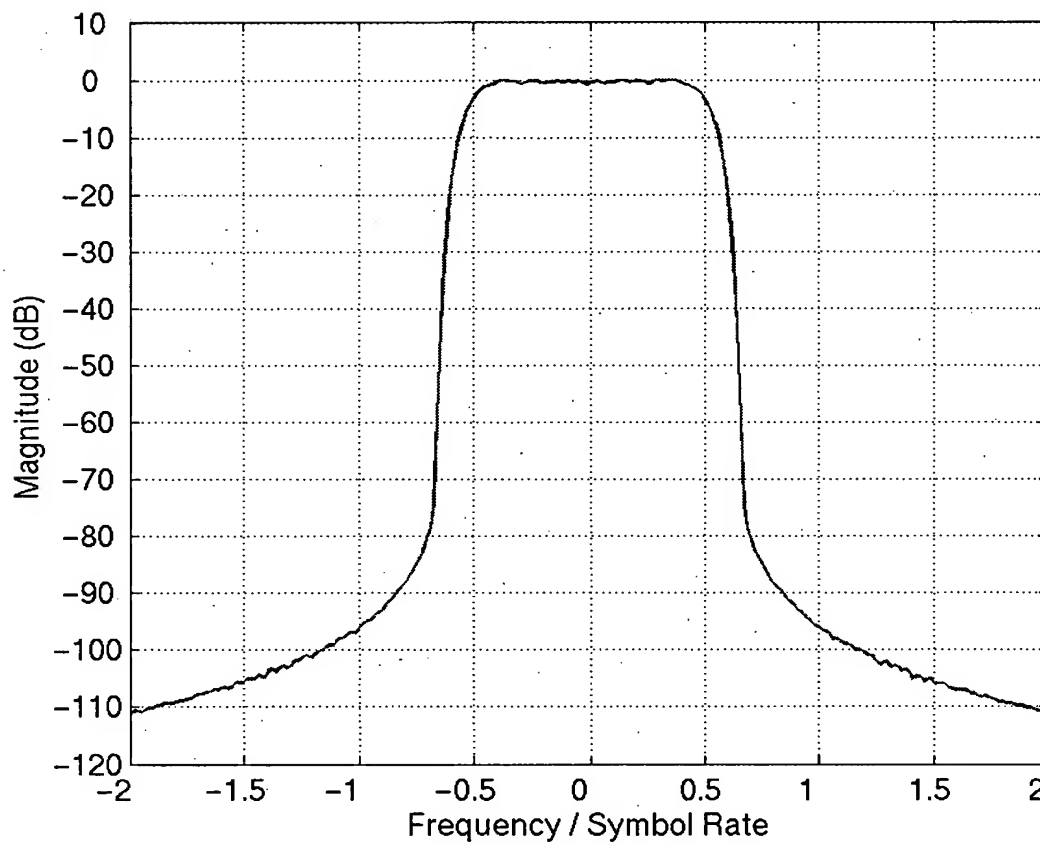
Figure 14 Estimated PSD of a conventional QPSK signal and the same signal after application of the exact hole-blowing method.
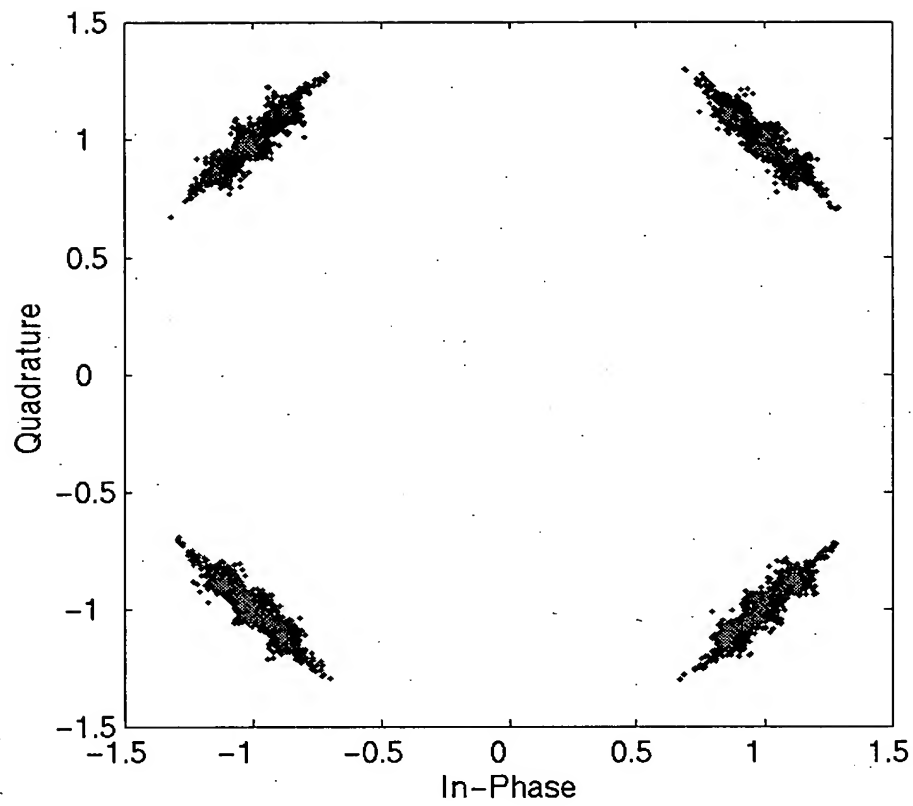
Figure 15a. I-Q plot of the modified signal after demodulation, showing that some distortion has been introduced into the signal. The measured RMS EVM is 6.3%.
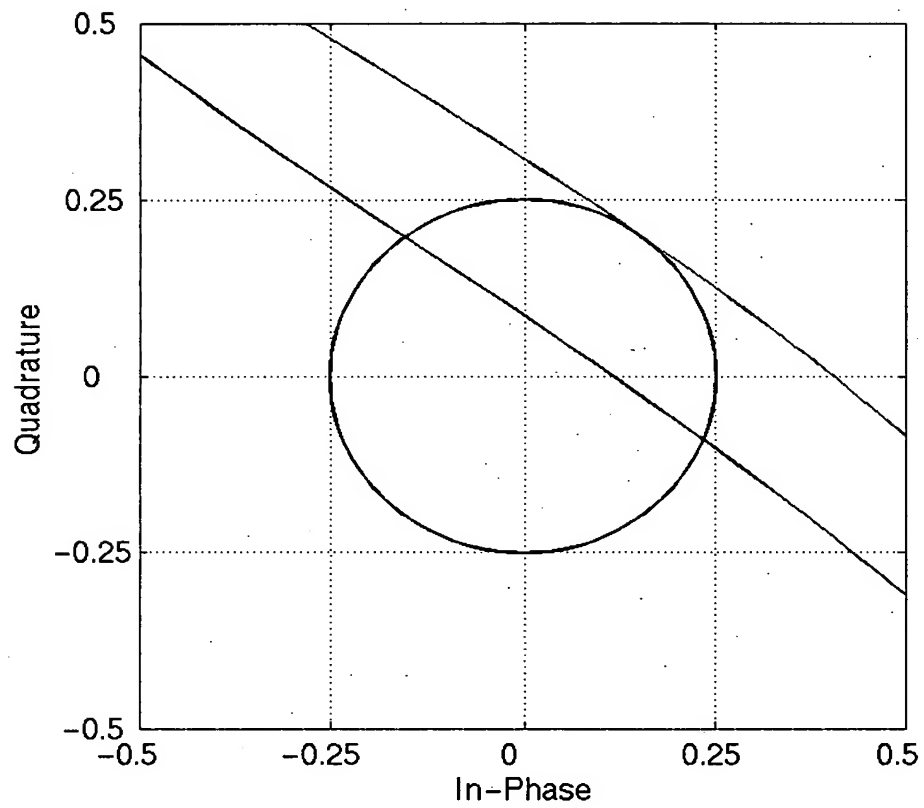
Figure 15b. Demonstration of non-linear filtering using a root-raised cosine pulse that is the same as the pulse-shaping pulse.
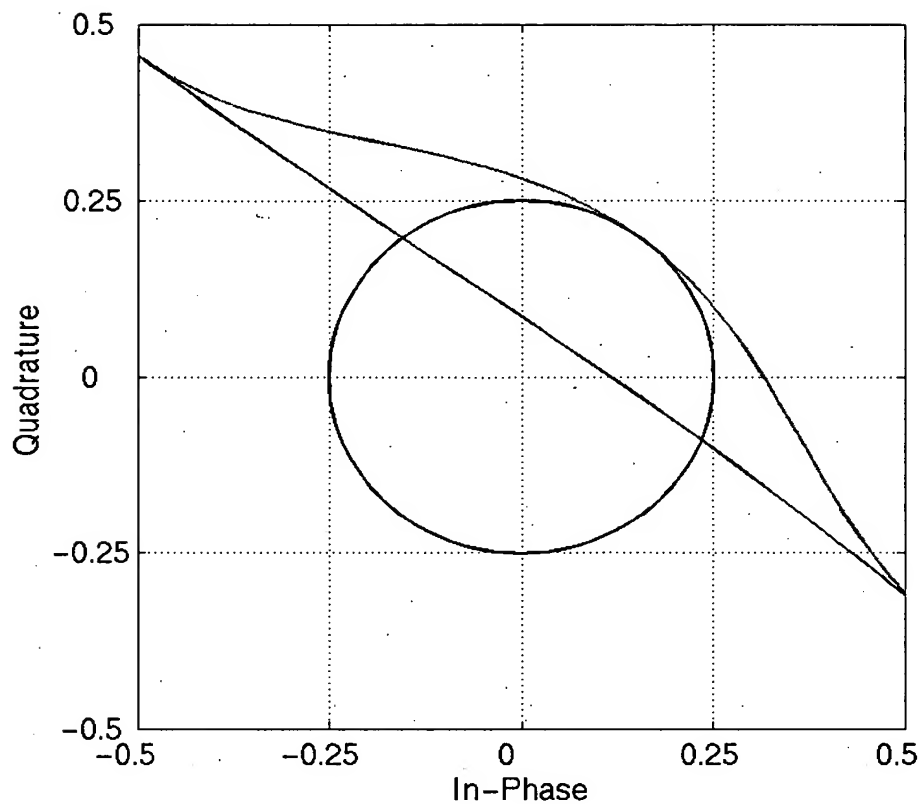
Figure 15c. Demonstration of non-linear filtering using a Hanning window for the correction pulse, with the time duration equal to ½ the symbol duration.
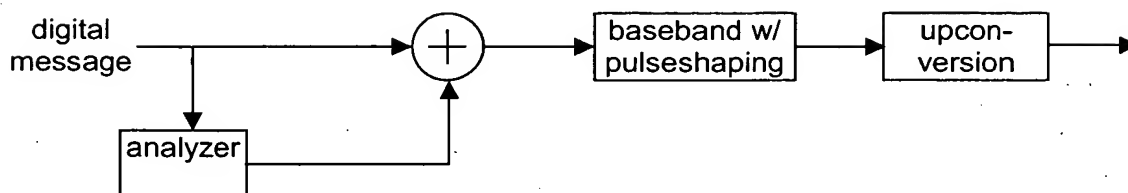

Figure 16a. **Alternative modification of generic PAM generator to include present invention.**
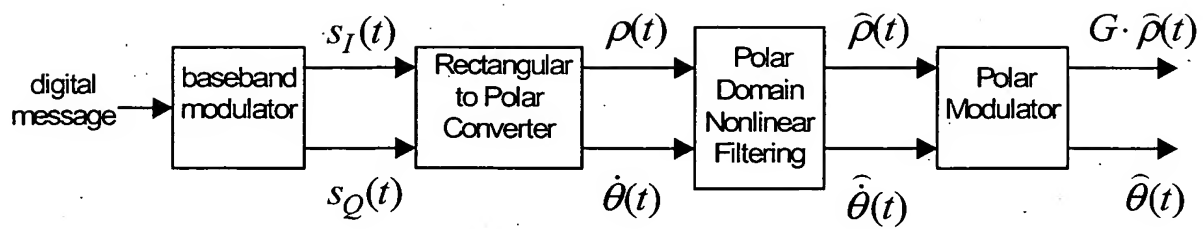
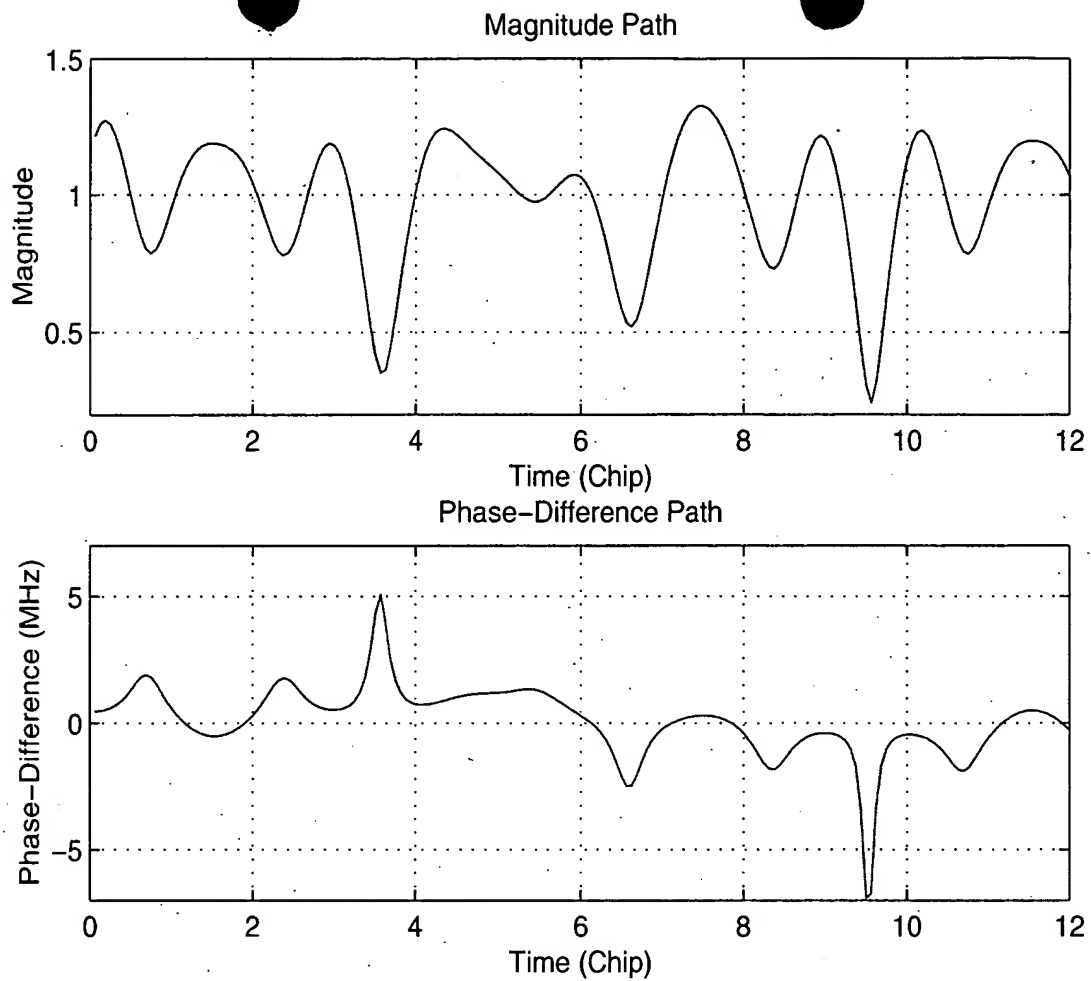**Figure 17a.** Schematic for polar domain nonlinear filtering

Figure 18. The above plot shows the magnitude component of the polar coordinate signal. The plot below shows the difference of the phase component of the polar coordinate signal.
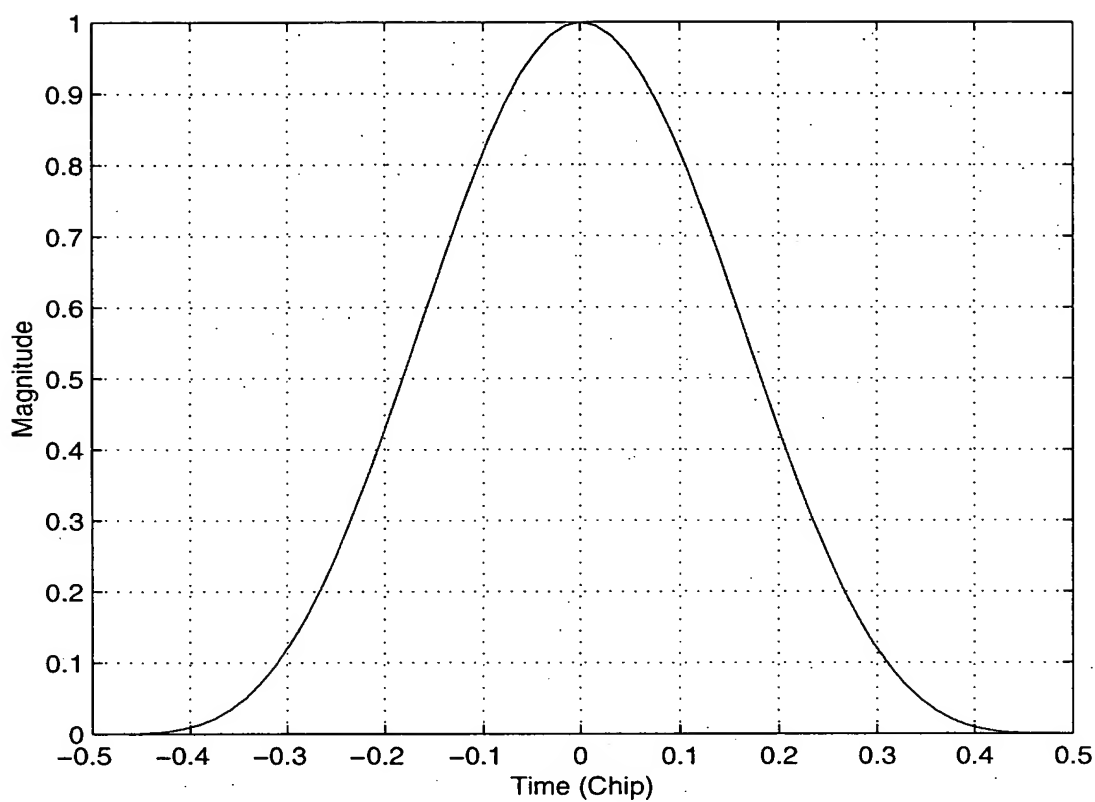
Figure 19. Impulse response of a DZ3 pulse. The impulse response of the pulse is defined in McCune's paper entitled "The Derivative-Zeroed Pulse function Family."
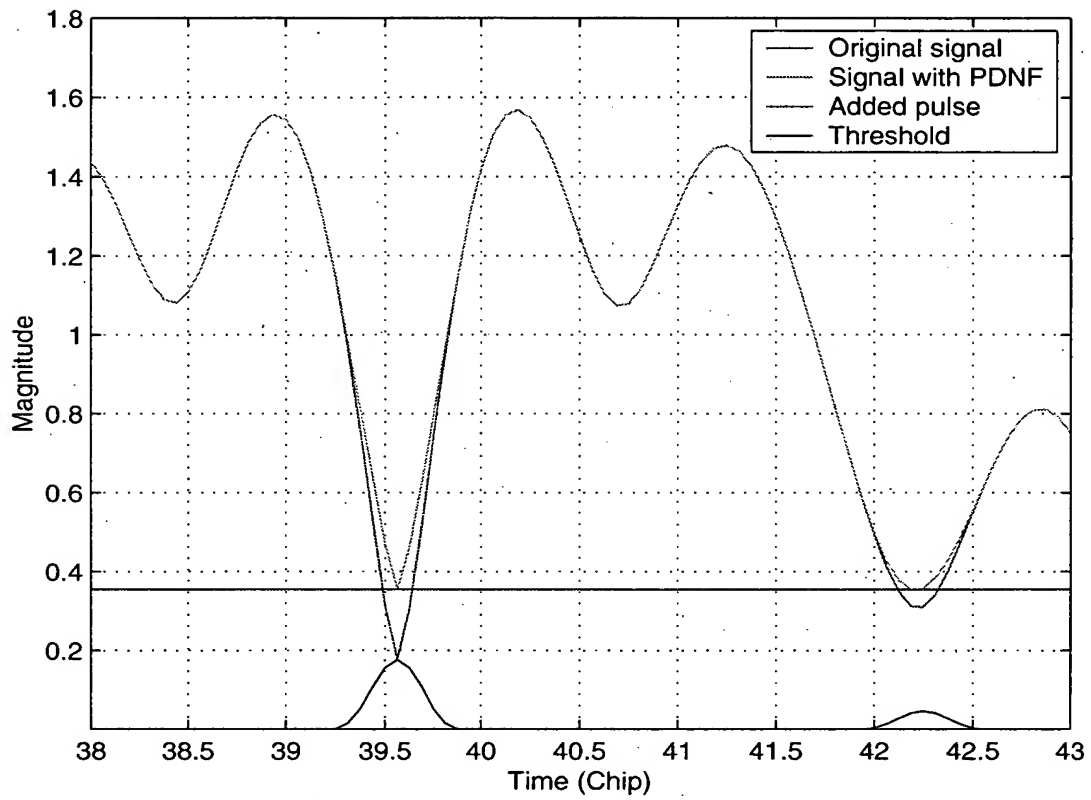
Figure 20. The red line is the original magnitude component before polar domain nonlinear filtering. The green line is the magnitude component after the polar domain nonlinear filtering. The blue line is the threshold and the back pulses are the pulses added to the magnitude component.
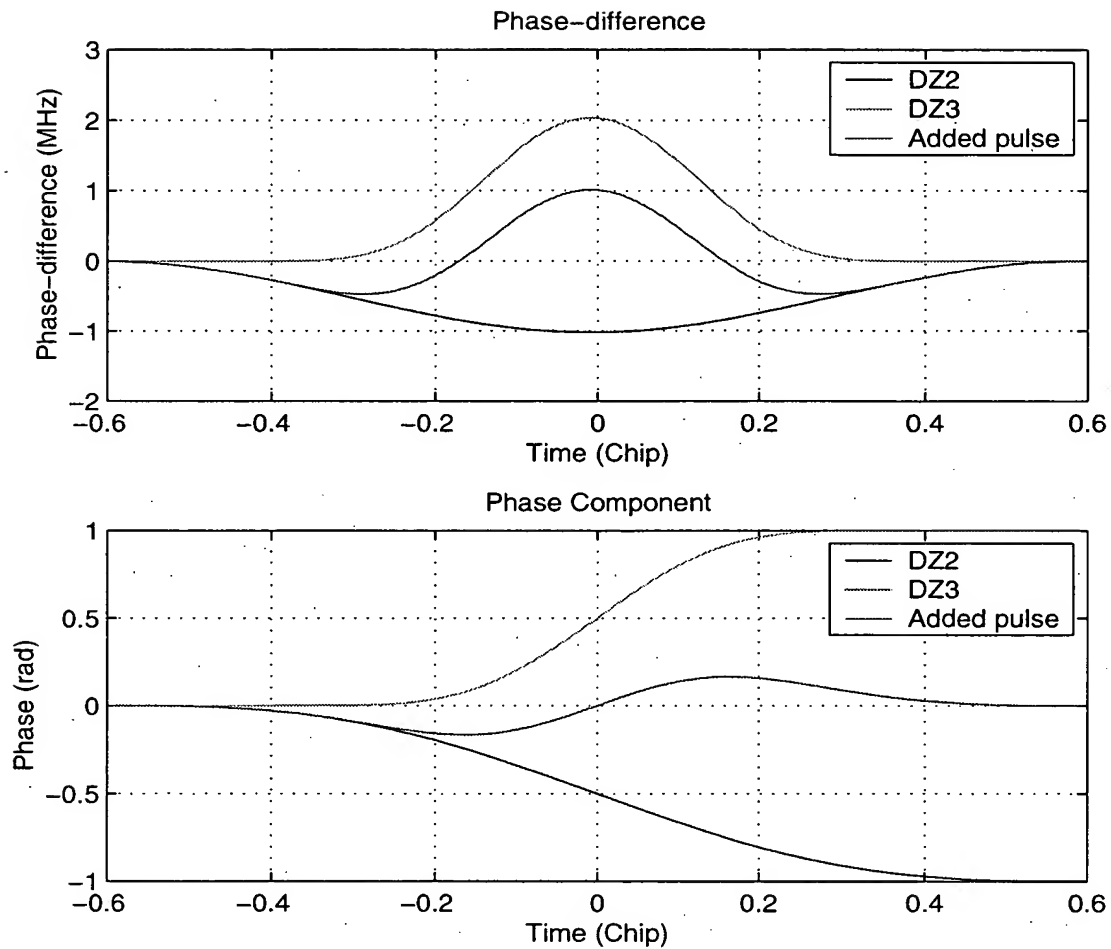
Figure 21. The above plot shows an example of the pulse (red pulse) inserted to the phase-difference path. The added pulse is composed of two pulses (green and blue pulses) with different sign but same integration area. Therefore, the integration of the red pulse over time is zero. The lower plot shows the effect of nonlinear filtering on the phase trajectory. The modified phase trajectory first deviates and then merges back to the original phase trajectory.
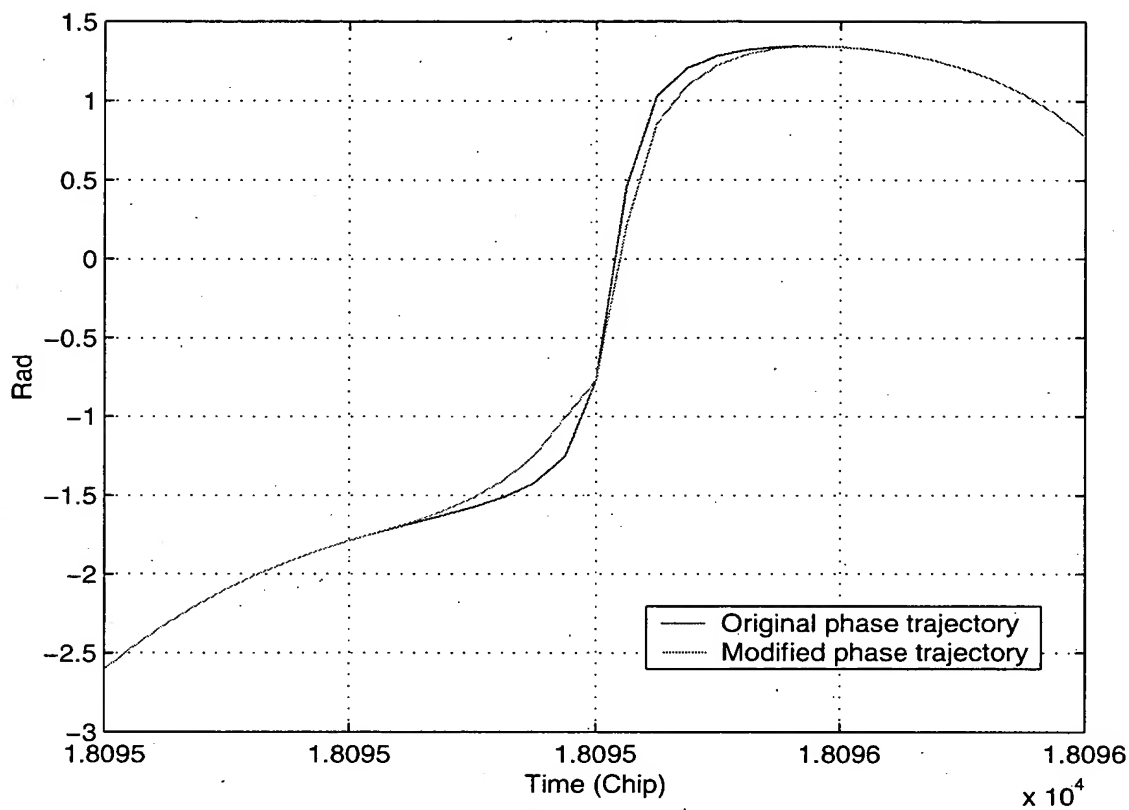
Figure 22. The phase trajectory before and after the nonlinear filtering of phase component.
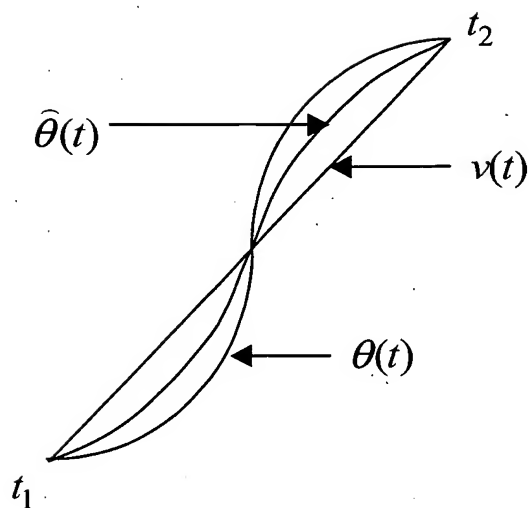
Figure 23. An alternate way for nonlinear filtering of the phase component in a polar coordinate system.
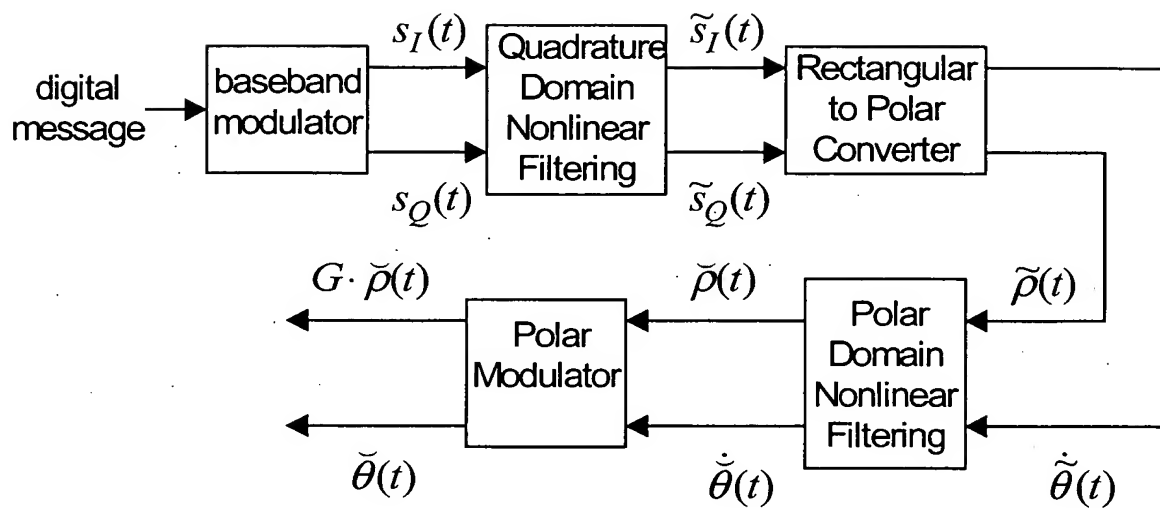
Figure 24. The block diagram for the concatenated system of nonlinear filtering in both quadrature and polar domain.
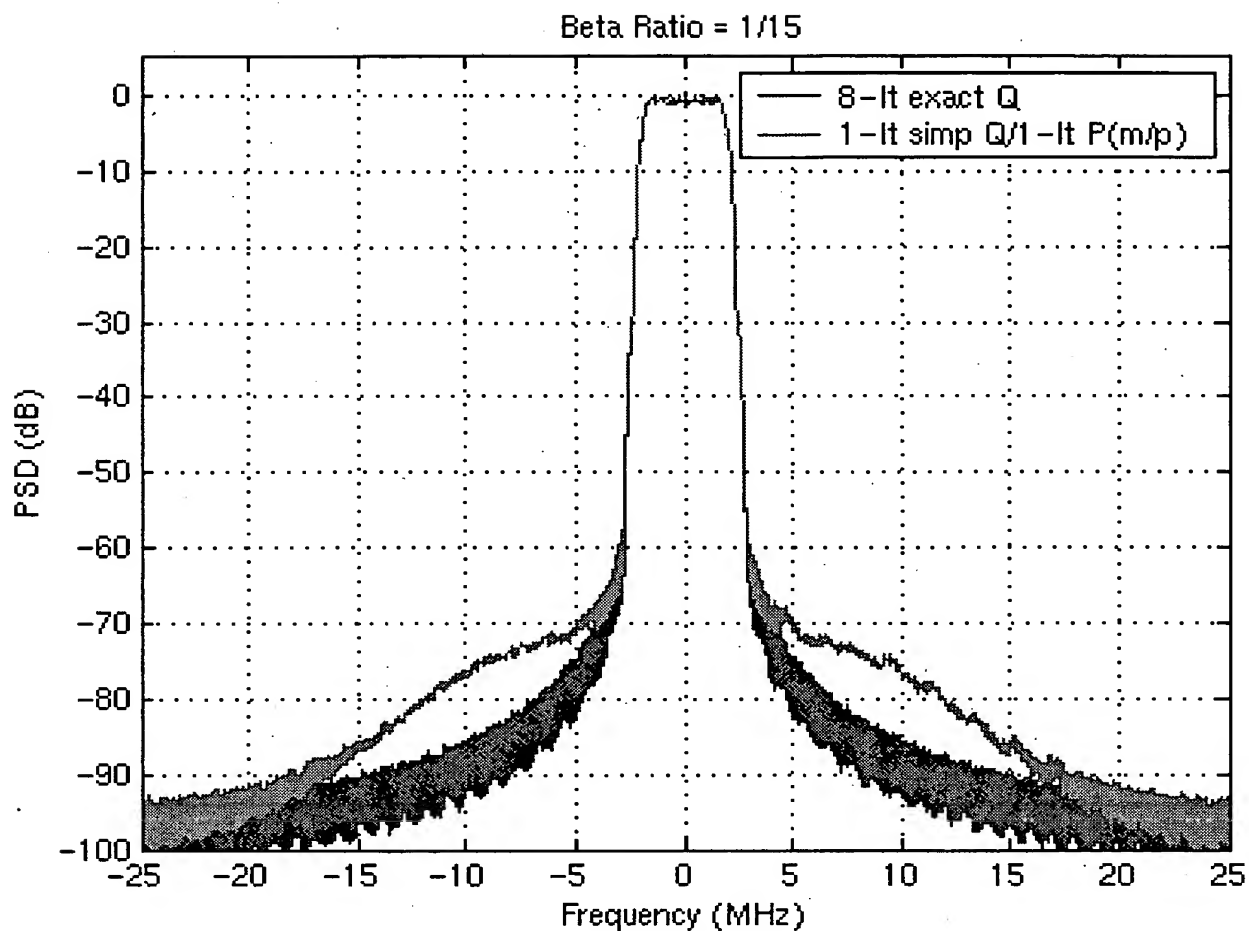
Figure 25. Blue curve represents the signal with 8-iterations of quadrature domain nonlinear filtering. Red curve represents the signal with 1-iteration of quadrature domain nonlinear filtering followed by a polar domain nonlinear filtering. The spectral re-growth is limited below −60 dB. In addition, good spectral roll-off is achieved.
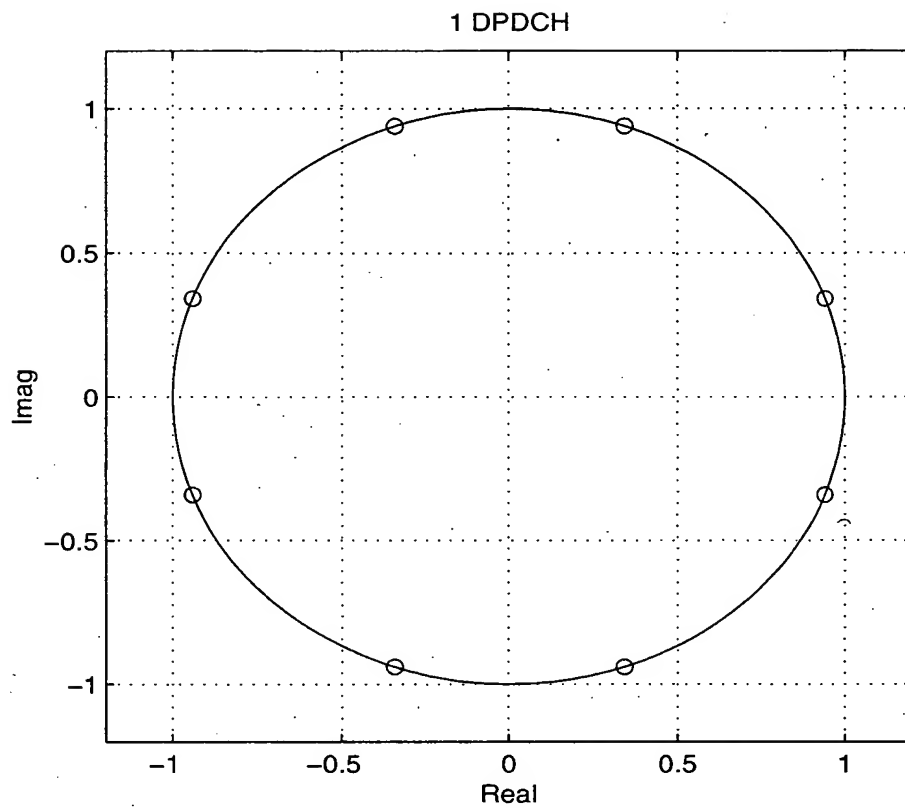
Figure 26 I-Q plot for the UMTS signal constellation with one active data channel and a beta-ratio of 7/15.

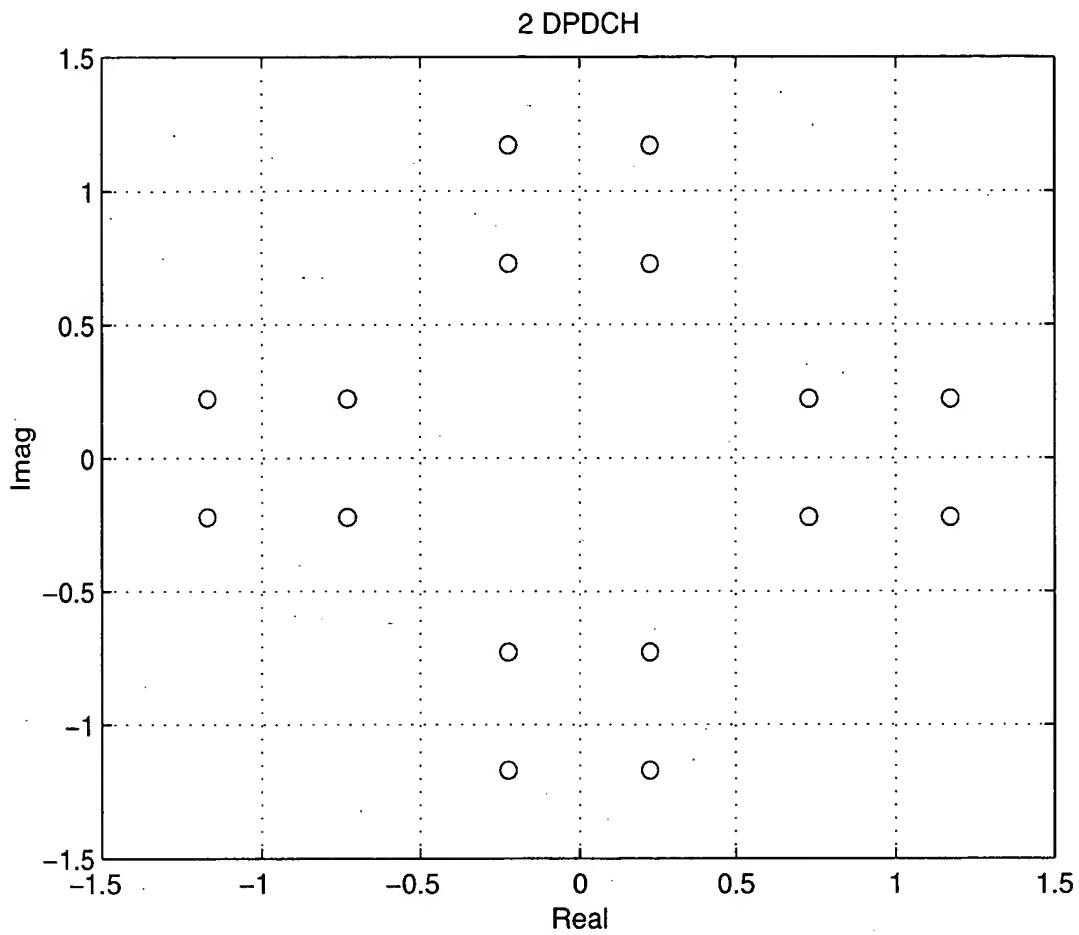**Figure 27** I-Q plot for the UMTS signal constellation with two active data channels and a beta-ratio of 7/15.

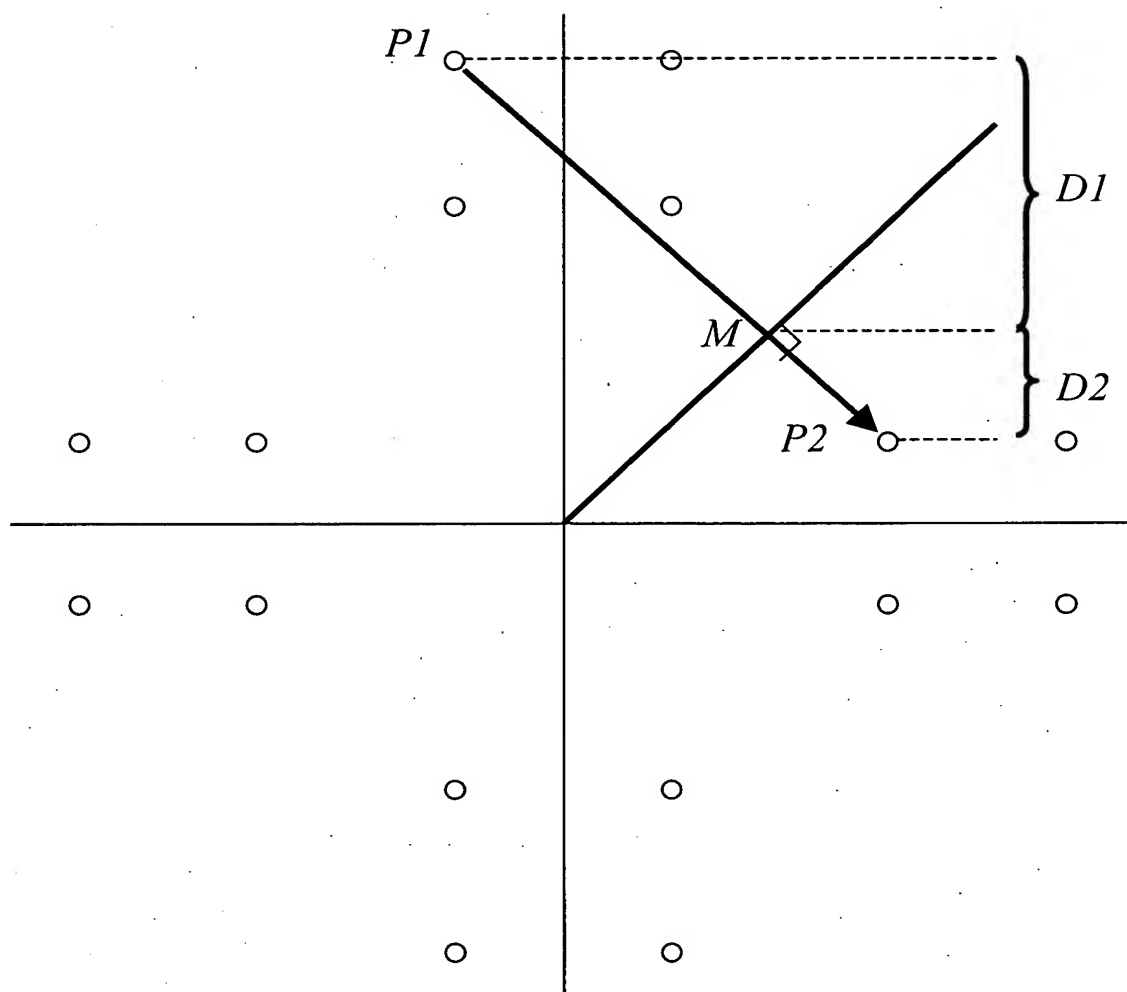**Figure 28a** Algorithm for finding the timings of the low-magnitude events.
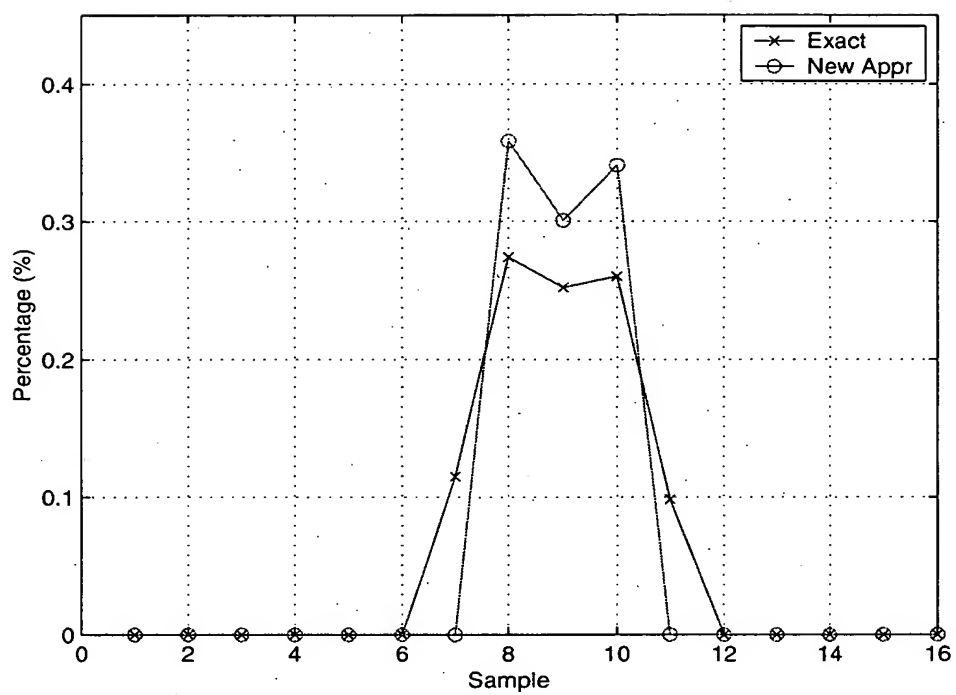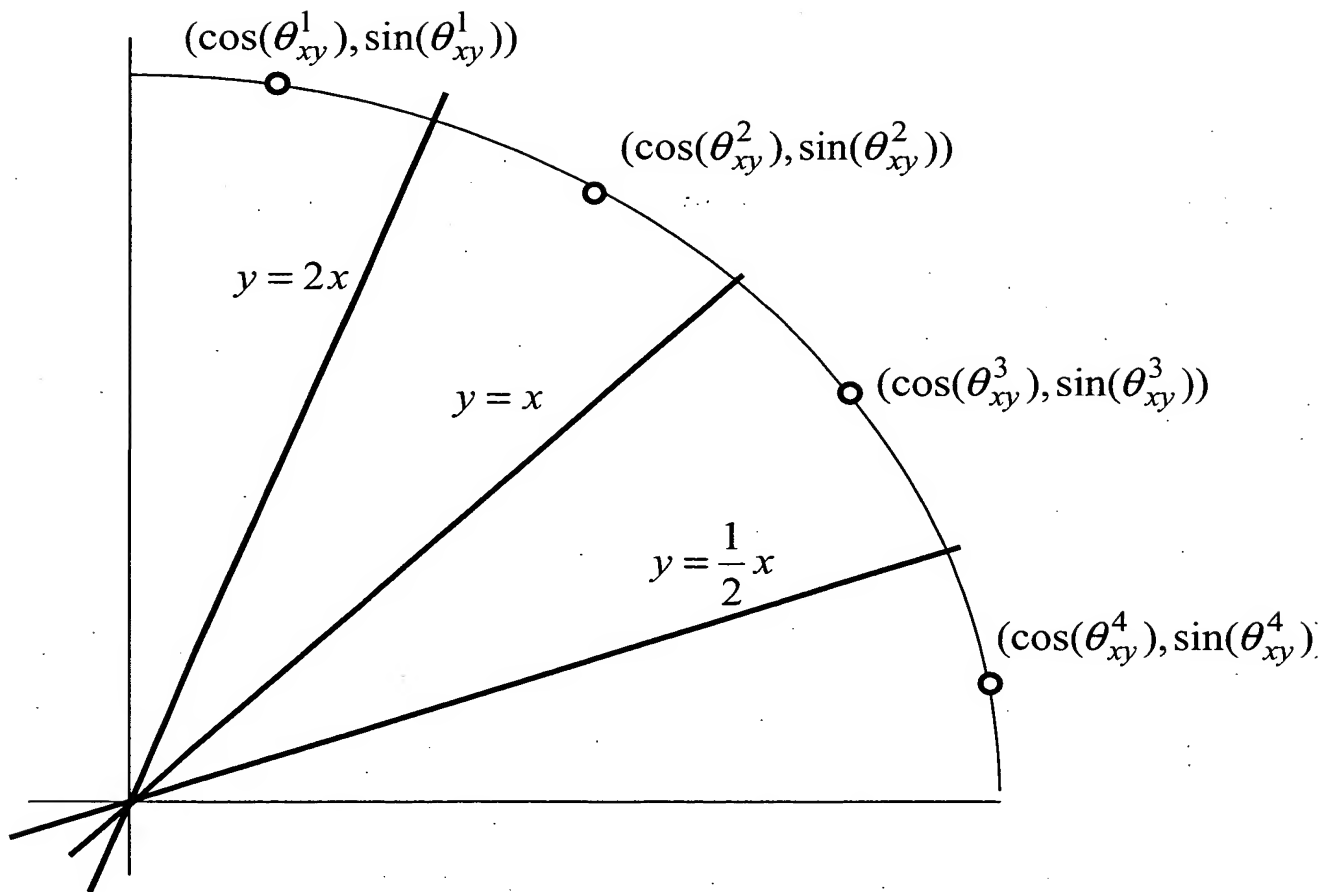
Figure 28b

Figure 29 An I-Q plot to illustrate the algorithm of line-comparison method. These lines with different slops partitioned the first quadrant into several sub-sections. Each sub-section is represented by a pre-stored value.

$$(|\Delta x|, |\Delta y|) \qquad (|\Delta x|_0, |\Delta y|_0) \qquad (|\Delta x|_1, |\Delta y|_1) \qquad (|\Delta x|_2, |\Delta y|_2)$$

The vector is rotated clockwise by an angle equal to

The vector is rotated clockwise by an angle equal to

The vector is rotated counterclockwise by an angle equal to

$$\Theta_0 = \tan^{-1}(1) \qquad \Theta_1 = \tan^{-1}(1/2) \qquad \Theta_2 = \tan^{-1}(1/4)$$
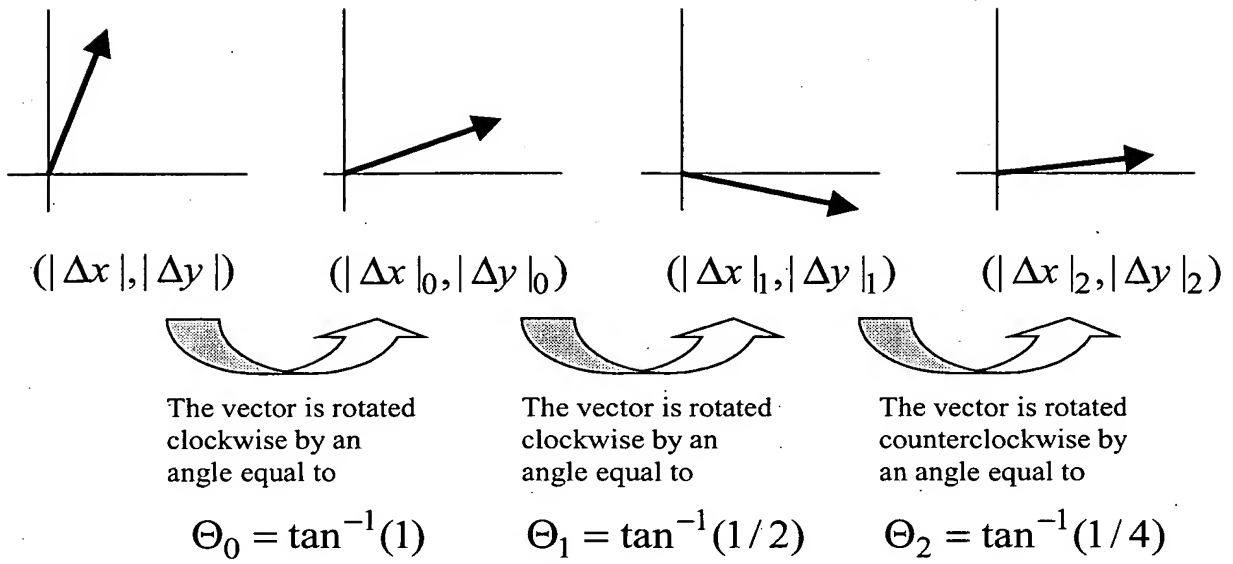
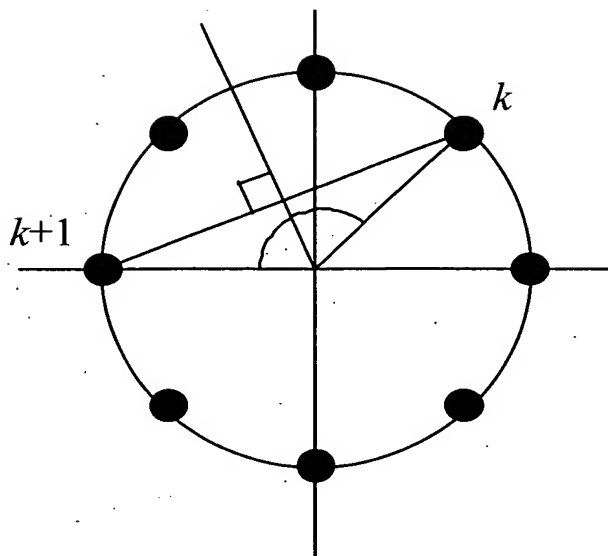**Figure 30** The CORDIC-like algorithm for vector quantization

Figure 31 Illustration of the method used to calculate the phase of the corrective pulse(s) in patents 5,805,640 and 5,696,794. The signal transitions from symbol k to symbol k+1. The so-called phase rotation in this example is $\pi-\pi/4 = 3\pi/4$. The phase of the correction pulse(s) is thus $\pi/4 + 3\pi/8 = 5\pi/8$. The correction vector is orthogonal to a straight line drawn between symbols k and k+1.
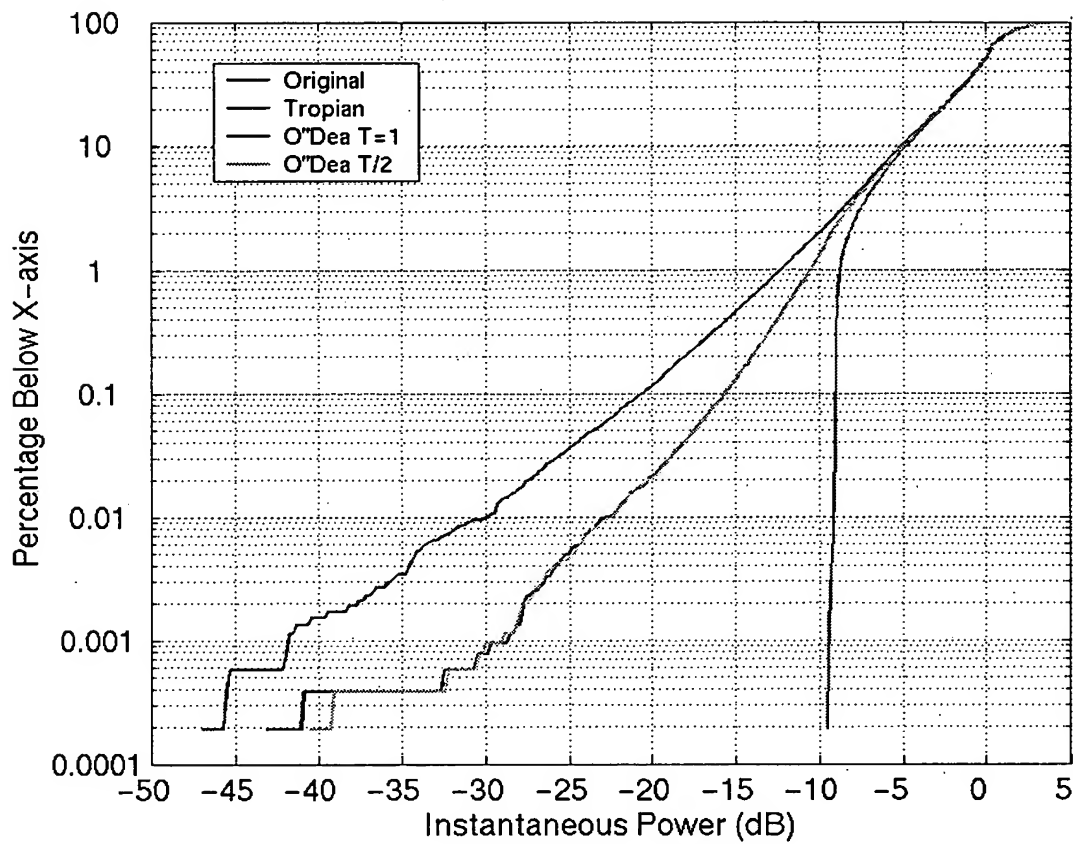
Figure 32 Cumulative Distribution Functions (CDF) obtained with the Tropian method and the two O'Dea methods when the signal is π/4 QPSK with raised cosine pulse-shaping and excess bandwidth of 22%. The desired minimum power is 9 dB below RMS.
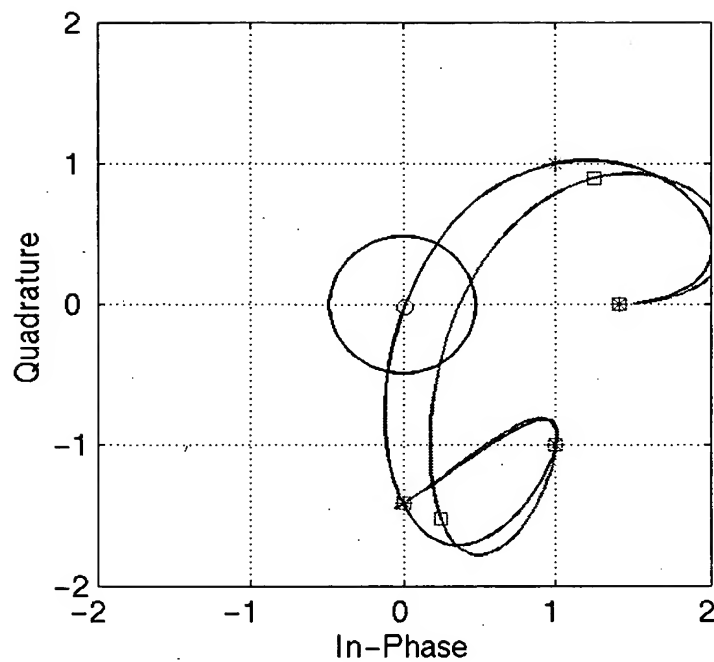
Figure 33 Example where the O'Dea symbol rate method works fairly well. The original signal envelope is shown in blue, and the modified envelope is shown in red. The sample used to calculate the correction magnitude is indicated with a 'o'.

Figure 34 Example where the O'Dea symbol rate method performs poorly. The original signal envelope is shown in blue, and the modified envelope is shown in red. The sample used to calculate the cor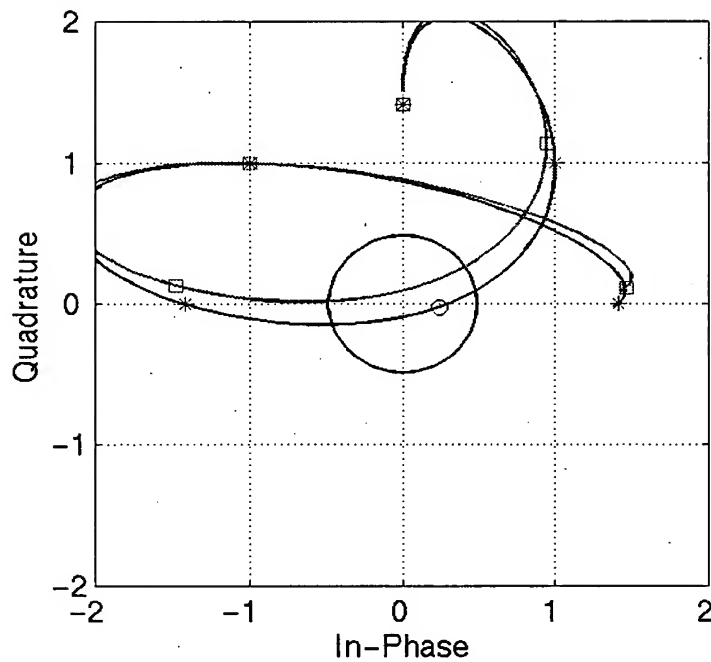rection magnitude is indicated with a 'o'. This example shows error both in the phase of the correction (incorrect sign), and in the magnitude.

Figure 35 Example where the O'Dea T/2 method performs poorly. The original signal envelope is shown in blue, and the modified envelope is shown in red. The sample used to calculate the correction magnitude is indicated with a 'o'. This example shows error both in the phase of the correction (incorrect sign), and in the magnitude.
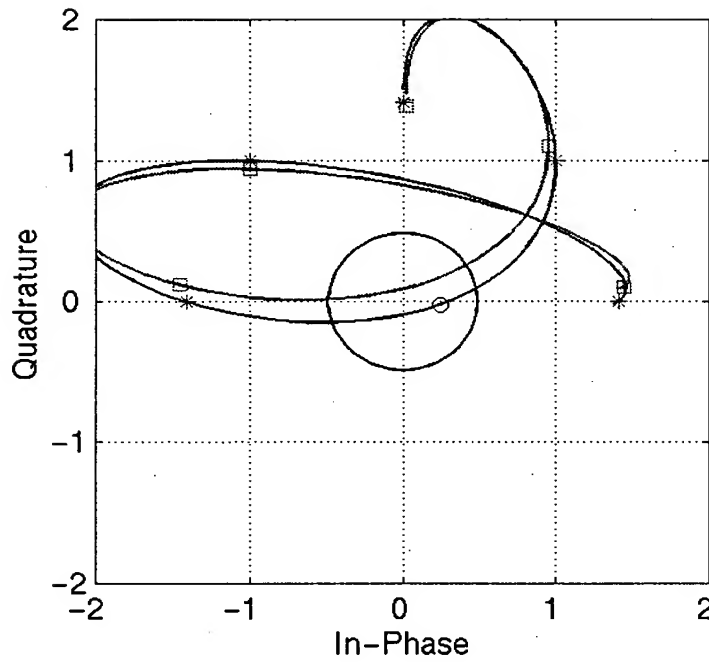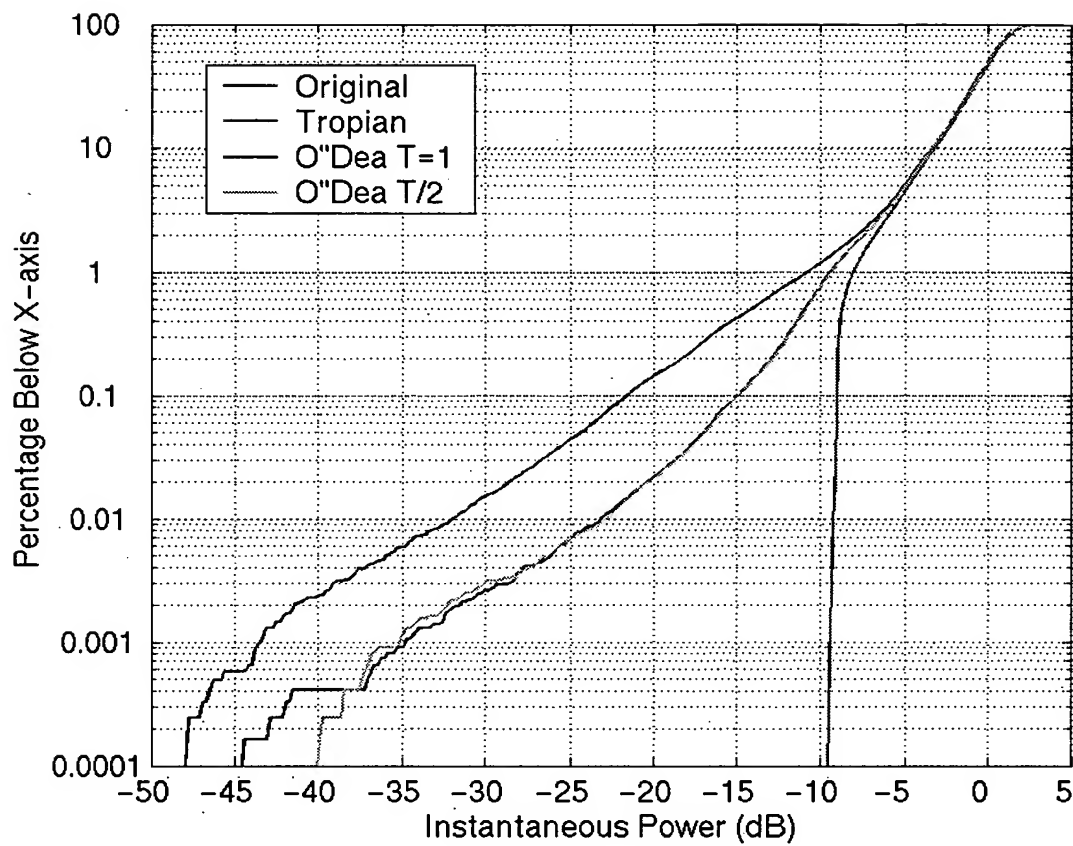
Figure 36 Cumulative Distribution Functions (CDF) obtained with the Tropian method and the two O'Dea methods when the signal is a 3GPP uplink signal with 1 active DPDCH and amplitude ratio of 7/15. The desired minimum power is 9 dB below RMS.
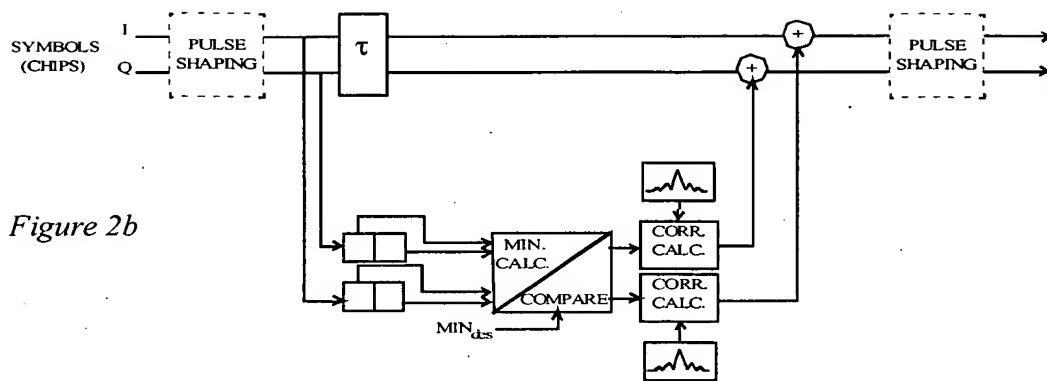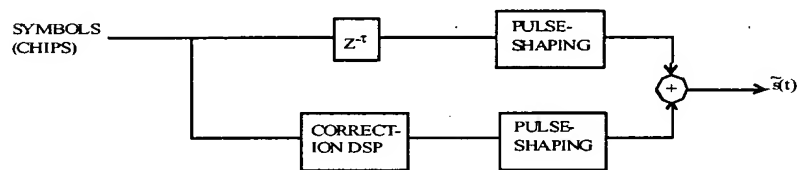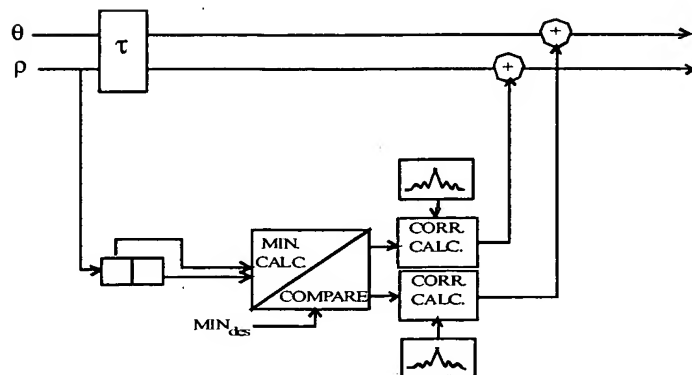
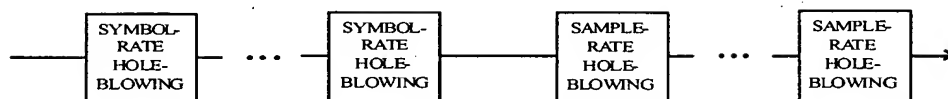Figure 2b

Figure 16b

Figure 17b

Figure 16c ────→ | SYMBOL-RATE HOLE-BLOWING | ··· | SYMBOL-RATE HOLE-BLOWING | ────→

Figure 16d ────→ | SAMPLE-RATE HOLE-BLOWING | ··· | SAMPLE-RATE HOLE-BLOWING | ────→

Figure 16e ────| SYMBOL-RATE HOLE-BLOWING | ··· | SYMBOL-RATE HOLE-BLOWING | | SAMPLE-RATE HOLE-BLOWING | ··· | SAMPLE-RATE HOLE-BLOWING | ────→